CNRS
Centre National
de la Recherche Scientifique

INFN
Instituto Nazionale
di Fisica Nucleare

Power and timing calibration of the Photon Calibrator for VSR2

Timothée Accadia, Loïc Rolland, Benoît Mours

VIR-0404A-10

July 1, 2010

Abstract

To operate an interferometric gravitational waves detector like Virgo one need is to reconstruct the differential motion of its mirrors. The reconstruction could be characterized by inducing a calibrated displacement on one mirror and compare it with the reconstructed h(t) signal. This can be achieved by acting on a mirror through electromagnetic actuators (main method) or by pushing one mirror with the radiation pressure from an auxiliary laser. The setup needed to achieve the last method is what we call the Photon Calibrator (PCal). Its description and calibration is the purpose of this note. Section 1 concerns the principle of the PCal. Section 2 presents the apparatus used in the Virgo experiment: the location, its components and their characteristics. Section 3 deals first with the power calibration of the monitoring photodiode including results of two calibrations performed before and after VSR2 (May 2009- January 2010). Section 4 is dedicated to the timing of the monitoring photodiode.

Contents

1 Principle of the Photon Calibrator

When a flux of photons hits a mirror, reflected photons transfer momentum to it by recoil and create a force F perpendicular to its surface. This force is proportional to the reflected power P_{ref}, the cosine of the beam incident angle i and the speed of light in vacuum c:

$$F = \frac{2\cos i}{\mathrm{c}} P_{ref} \tag{1}$$

In this note, we assume that the mirror reacts like a rigid body and limitations of such model are discussed in the note on the h-reconstruction checks (see [1]).

For a sinusoidal power line applied on the mirror center whose the frequency is much greater than the pendulum resonnant frequency (0.6 Hz), Virgo suspended mirrors act like free falling masses and the induced longitudinal displacement is given by the equation 2 where m is the mass of the mirror, P_{ref} is the amplitude of the sinusoidal power reflected and f its frequency. Note that the reflected and injected powers are linearly linked with the mirror reflection factor which is dependant of the laser wavelength and the beam incident angle.

$$\Delta L_{pend} = -\frac{1}{m(2\pi f)^2} \frac{2\cos i}{c} P_{ref} \tag{2}$$

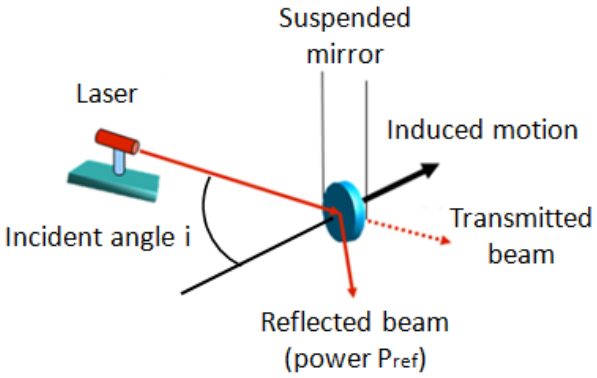

Figure 1: Principle of the PCal used in Virgo

2 Experimental setup

2.1 Location and general geometry

Two PCals are located on the input of the North and West arm but only the first one has been installed and calibrated for VSR2 (see figure 2). A laser diode located in the DAQ room produces light which is propagated by an 30 meters length optical fiber until a 30×30 cm injection bench. The beam coming from the injection bench goes inside the vacuum tower via the Upper North West (NWU) viewport (VP). The reflected and transmitted beams can be sensed respectively behind the Down North East (NED) and Down South East (SED) VP. No output bench was installed for VSR2.
The optical bench has an angle of 16° with respect to the horizontal plane in order to target the mirror center. The beam being parallel and 10 cm above the bench level, the impact angle on the mirror surface has been estimated to 40.88° with an uncertainty of 1° (source [2], see figure 3 to visualise the plane defined by the three beams in red oriented lines on the figure and see figure 4 for the dimensions).
On the injection bench (figure 5), the laser beam is first collimated. 99% of the beam power is sent by a high reflectivity mirror M in direction of the mirror. The 1% left is sensed by a photodiode used to monitor the laser beam, read and stored in the channel *Ca_NI_PCal*.

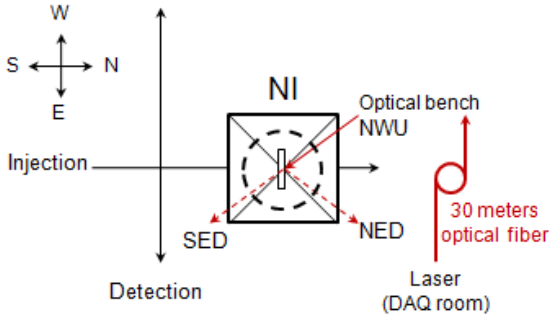

Figure 2: Location of the pcal at the input of Virgo north arm.

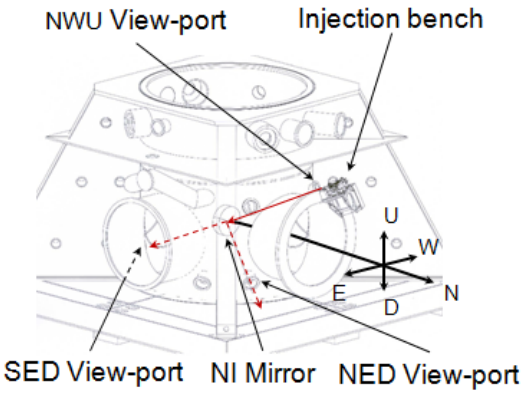

Figure 3: View of the pcal beams plan.

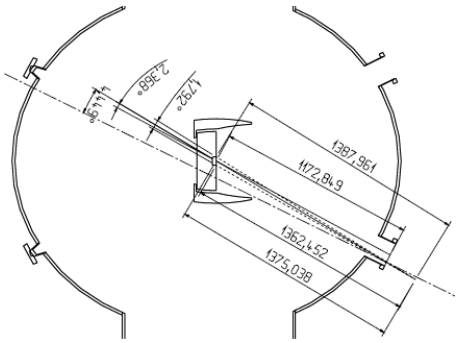

Figure 4: Distance in mm between the NI mirror and reflection VP in the beam plane, source [2]

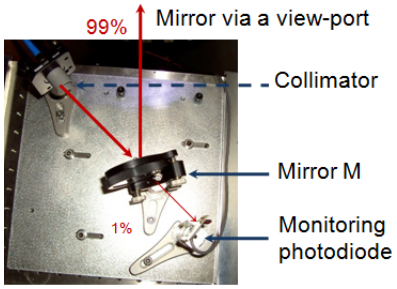

Figure 5: Picture of the optical set up on the injection bench.

2.2 Laser beam properties

The laser diode (model SFA_100_915_D2_01 which datasheet is available on [4]) has a wavelength of 915 (±5) nm. It can produce a maximal power of 1.2 Watt. The radius of the laser beam after collimation (collimator Thorlabs, see [4]) has been measured at three positions on an optical bench at LAPP (see table 1 for the measured values). A linear ajustement on previous data gives the following equation:

$$r(z \text{ in mm}) = 1.5(\pm 1.8)mm + 3.75(\pm 1) \times z \times 10^{-3} \quad (3)$$

With the last relation, we calculate the laser beam radius at injection-reflection-transmission VP and at the position where the incident beam hits the mirror. They are given in table 2.

z (mm)	r(z)(mm)
0.0	1.25 ± 2
1500.0	7.5 ± 2
3000.0	12.5 ± 2

Table 1: Measurements of the beam radius at different distance z to the laser output at LAPP.

Location	$\mid z \mid$ [mm]	r [mm]
VP-injection	320 ± 50	2.7 ± 1.8
Mirror	1493 ± 50	7.1 ± 2.3
VP-reflection	2666 ± 50	11.5 ± 3.2
VP-transmission	2746± 50	11.8 ± 3.3

Table 2: Distance z from the laser output and beam radius r at interesting positions in NI tower.

2.3 Laser drive and incident beam monitoring

The power modulation is directly controlled by an external excitation signal driving the laser power supply and coming from the *Ca_NI_Photon* channel via a DAC with a 3.7 kHz anti-image cut-off frequency. The incident beam is sensed by a photodiode (cf. figure 5 and table 3 for its characteristics) which converts the power received into a current . This current is then converted in voltage by an analog readout electronics and stored in the channel *Ca_NI_PCal* at 20 kHz via an ADC.

The laser power linearity relative to the *Ca_NI_Photon* level has been ckecked in DC mode behind the transmission VP: the laser beam power has been measured for different injected level, with the powermeter (see next section for a description of the setup) and the photodiode during 60 seconds. Figure 6 shows powermeter level against *Ca_NI_Photon* and *Ca_NI_PCal* respectively on the top and down plots. The residuals between powermeter and photodiode level is superimposed on right plot. Since saturation is seen in powermeter channel relatively linear with the photodiode (residuals inferior to 2%), it indicate that it is the laser that saturates. The following constraints on injected amplitudes are derived:

$$1.0V < Ca\_NI\_Photon < 3.5V \tag{4}$$

Active area	10×10 mm
Maximum power dissipation	100 mW
Photosensitivity	0.56 A/W at 915 nm
Cut-off frequency	> 1 MHz

Table 3: S3590-01 photodiode characteristics.

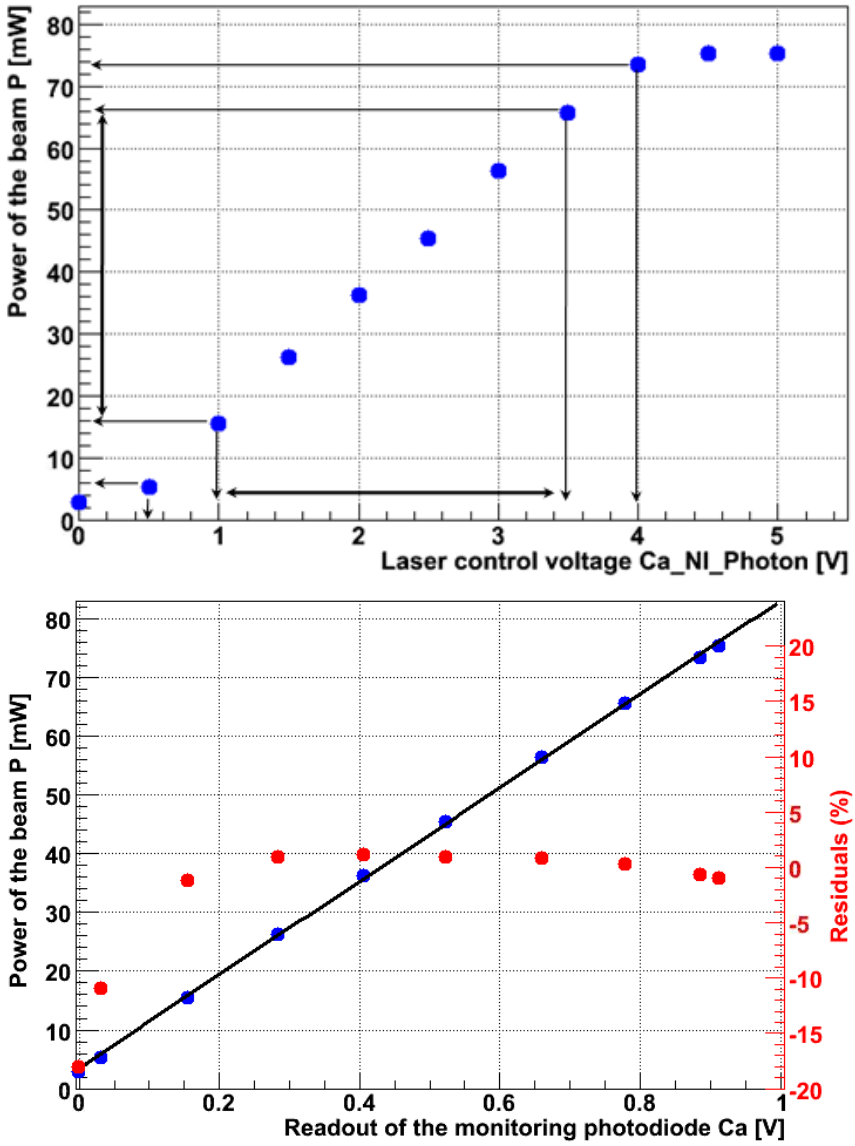

Figure 6: Laser power linearity checked with the powermeter and the photodiode. On the top plot, is represented the PCal beam power measured P with the powermeter against *Ca_NI_Photon* (bold arrows show the non-saturation range). On the down plot, Power P is represented vs Photodiode level Ca in blue points and the residuals relative to the black fitted line are given in red points.

2.4 Measurement of VP transmitivity

The knowledge of the VP transmitivity is crucial to know the beam power inside the tower P while it is measured outside P'. The power transmitivity (and reflectivity) coefficients for the three VPs have been measured before their installation on an optical bench with the PCal laser (see figure 7). Because we have an uncertainty on the position where the PCal laser is going through the VP, we measured positions along two orthogonal directions for each side to check the uniformity. We tested also the incident angle dependance (few degrees around 10°) but no variation were observed. The RMS of measurements for each VP is used as errors and because they are small for the three VPs, they can be considered uniform. Average values and the associated RMS of VPs transmitivity and reflectivity are given in table 4. The losses L are defined as $1-T-R$ where T and R are respectively the transmitivity and reflectivity mean coefficients for one VP. Because we don't know where the power is lost (at the reflection or the transmission), the transmission coefficients is at least what we have measured T and at most T + $\frac{L}{2}$. Therefore, T is symmetrized by adding half of the losses.

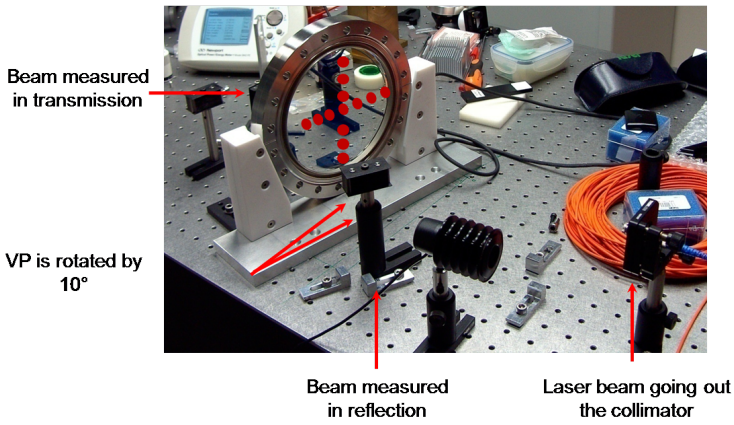

Figure 7: View of the experimental setup used to measure the VPs transmitivity.

View-port	transmission (%)	reflection (%)	losses (%)	transmission symmetrized (%)
Injection	98.66 ± 0.11	0.61 ± 0.03	0.73	99.03 ± 0.47
Reflection	99.0 ± 0.14	0.53 ± 0.03	0.47	99.24 ± 0.38
Transmission	98.96 ± 0.1	0.71 ± 0.04	0.33	99.13 ± 0.26

Table 4: Power transmission and reflection coefficients of View-ports measured with the PCal laser (915nm) at an incident angle of 10°). The losses are also given.

3 Power calibration

The aim of the power calibration is to estimate the power reflected (cf. equation 2) by the North Input mirror (P_{ref}) from the photodiode readout *Ca_NI_PCal*. In addition, the power injected and transmitted (P_{inj} and P_{tra}) are measured. This procedure allows to perform a consistancy check in order to estimate systematic errors related to power losses.
In this section we present first the setup used to measure beam powers, then a description of the calibration procedure is describe and finally, the results of the two calibrations performed in May 2009 (pre-run) and January 2010 (post-run) are given.

3.1 Powermeter setup

To measure beam powers, a thermopile sensor is used (Newport, model 818P-010-12) which is connected to a powermeter (Newport, model 842_PE). General characteristics are given in table 5 and a more detailed setup description is available on [4]. Both powermeter and sensor head has been bought in October 2008. No recalibration was done in-between.

	Thermopile 818P-010-12	Powermeter 842_PE
Power range (W)	$[10^{-3}$ - $10^{1}]$	$[5.10^{-12}$ - 10^{4}]
Rise time (s)	0.5	1.0
Resolution ($\pm$.%)	2.5	0.5
Active area (cm^2)	1.13	-

Table 5: Thermopile sensor and powermeter specifications.

3.2 Measurements description and data analysis

The powermeter sensor is put between the mirror M and the input VP for the injection, after the output VPs for the reflection and transmission. For these two last VPs, the beam is firstly focalized with a 2 inches diameter lens with a 10 cm focal length to obtain a beam width smaller than the sensor aperture. Checks were made to verify that the lens losses are less than 1% and are estimated to 0.5 ± 0.5 %.
Before measuring the laser powers at one VP, the photodiode and powermeter offsets (Ca_0 and $P_0^{'}$ outside the tower) are measured by cutting the laser power with a beam dump.
Because we need to know the full power, the beam has to be entirely contained in the sensor head active area. In pratice, the beam is not perfectly centered on the sensor that is why the sensor can be moved along two orthogonal directions thanks to two motors (called M1 and M2 on figure 8). To measure the beam power, the sensor head scans the beam at 5×5 positions

with a 2 mm step(represented by black points on figure 8). In parallel the powermeter output, photodiode readout and motor positions are read and stored respectively in the channels *Ca_PowerMeter_Pwr* (1Hz), *Ca_NI_PCal* (20000Hz), *Ca_NSA_1_1_Pos* (1Hz) and *Ca_NSA_1_2_Pos*(1Hz).
For each position in the scan, a conversion factor $\alpha^{'}$ is computed (equation 5) between the laser beam power measured $P^{'}$ (not corrected by the VPs transmitivity) and the photodiode readout *Ca*, both corrected by their offsets. Note that the first three seconds of each positions measured have been removed due to the thermal response of {powermeter + sensor head} which is of the same order of magnitude (cf. row 2 of the table 5).

$$\alpha^{'} = \frac{P^{'} - P_0^{'}}{Ca - Ca_0} \quad \text{(W/V)} \tag{5}$$

Then a map representing the conversion factor in function of the motor positions is built (see figure 9). The map is fitted with a plateau-gaussian function which is defined in equation 6 and depends on five parameters { x_{center}, y_{center}, $R_{plateau}$, $\alpha_0^{'}$, w } .

$$\begin{aligned} \alpha^{'}(R) &= \alpha_0^{'} && \text{if } R < R_{plateau} \\ &= \alpha_0^{'} \exp^{-(\frac{R-R_{plateau}}{w})^2} && \text{else} \end{aligned} \tag{6}$$

where:

- $R = \sqrt{(x - x_{center})^2 + (y - y_{center})^2}$ is the distance a given position (x, y) to the position where the beam is centered on the sensor (x_{center}, y_{center}).
- $R_{plateau}$ is the distance for which the entire beam is inside the sensor.
- $\alpha_0^{'}$ (W/V) is the conversion factor inside the plateau.
- w is the width of the gaussian decay when the beam goes outside the sensor.

For each scan performed, a map is built and three conversion factors are extracted according the three following methods:

- the "fit" method which takes directly the fitted conversion factor $\alpha_0^{'}$.
- the "4 points" method which takes the four conversion factors from raw data of the four closest points to the plateau center (x_{center},y_{center}).
- the "1 point" method which takes the conversion factor from raw data of the closest point to the plateau center (x_{center},y_{center}).

These three methods are used to estimate systematic error introduced by the method choice. Conversion factors extracted at one VP with the same method but corresponding to different powers are averaged. One set of conversion factors ($\langle\alpha'_{inj}\rangle$,$\langle\alpha'_{ref}\rangle$,$\langle\alpha'_{tra}\rangle$) are then obtained per extraction method. Conversion factors are then corrected by the VPs and lens transmitivity to get the power inside the tower:

$$\alpha_{inj} = T_{inj}\left\langle\alpha'_{inj}\right\rangle \ , \ \alpha_{ref} = \frac{1}{T_{ref}\times T_{lens}}\left\langle\alpha'_{ref}\right\rangle \ , \ \alpha_{tra} = \frac{1}{T_{tra}\times T_{lens}}\left\langle\alpha'_{tra}\right\rangle$$

For a given set, the losses are obtained by comparing input and ouput powers inside the tower normalized by the reflected power:

$$Losses = \frac{P_{inj} - (P_{ref} + P_{tra})}{P_{ref}} = \frac{\alpha_{inj} - \alpha_{tra}}{\alpha_{ref}} - 1 \qquad (7)$$

Since there are three methods, three losses are computed. They are used to estimate the systematic errors on the power measurement. Because we don't know where losses occur (i.e at the input or output VPs), the reflected power is at least what has been measured P_{ref} and at most $P_{ref}(1+Losses)$. Therefore the reflection conversion factor α_{ref} at the mirror level is computed by adding half of the losses:

$$\alpha_{ref,sym} = \left[\alpha_{ref} + \frac{Losses}{2}\right] \quad \pm \quad \left[\frac{Losses}{2}\right] \qquad (8)$$

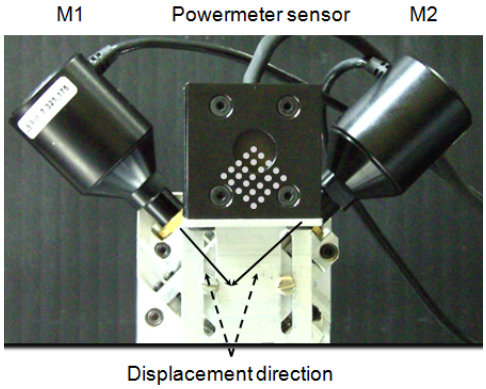

Figure 8: View of the powermeter sensor and its motorized support actuated by motors M1 and M2.

3.3 Calibration performed

The two calibrations presented here have been performed before the run in May 2009 and after in January 2010.

3.3.1 May 2009

The laser power level was controlled manually via a button on the front panel of the Laser Drive Box which value is given in the 4th column of table 6. Offsets P_0 and Ca_0 measured switching off the laser are also presented in table 6. In average, each position is measured during $11 - 3 = 8$ seconds. One typical map $\alpha^{'}(R)$ and the associated fitted function is shown figure 9 for each VP and fitted parameters are shown in table 9. At the injection and reflection, the beam goes outside the sensor at least on one edge and fits with the plateau-Gaussian function are pretty accurate. For the transmission, the beam stays inside which implies large errors on the center position fit. However the impact on the $\alpha_0^{'}$ value is small looking at its error and there is a small consequence on the 4 and 1 points methods since the selected points correspond to a beam inside the sensor head. Table 8 shows (α_{inj} ,α_{ref}, α_{tra}) for May 2009 and the corresponding Losses, for the three methods.

Measurement location	start GPS	Δt(s)	$P_0^{'}(mW)$	Ca_0(mV)
Injection	925723300	60	0.24±0.15	1.26±0.01
Reflection	925736880	60	-0.6±0.17	1.22±0.00
Transmission	925740239	60	0.03±0.16	1.26±0.01

Table 6: Powermeter ($P_0^{'}$) and Photodiode (Ca_0) offsets measured at the injection, reflection and transmission VPs in May 2009.

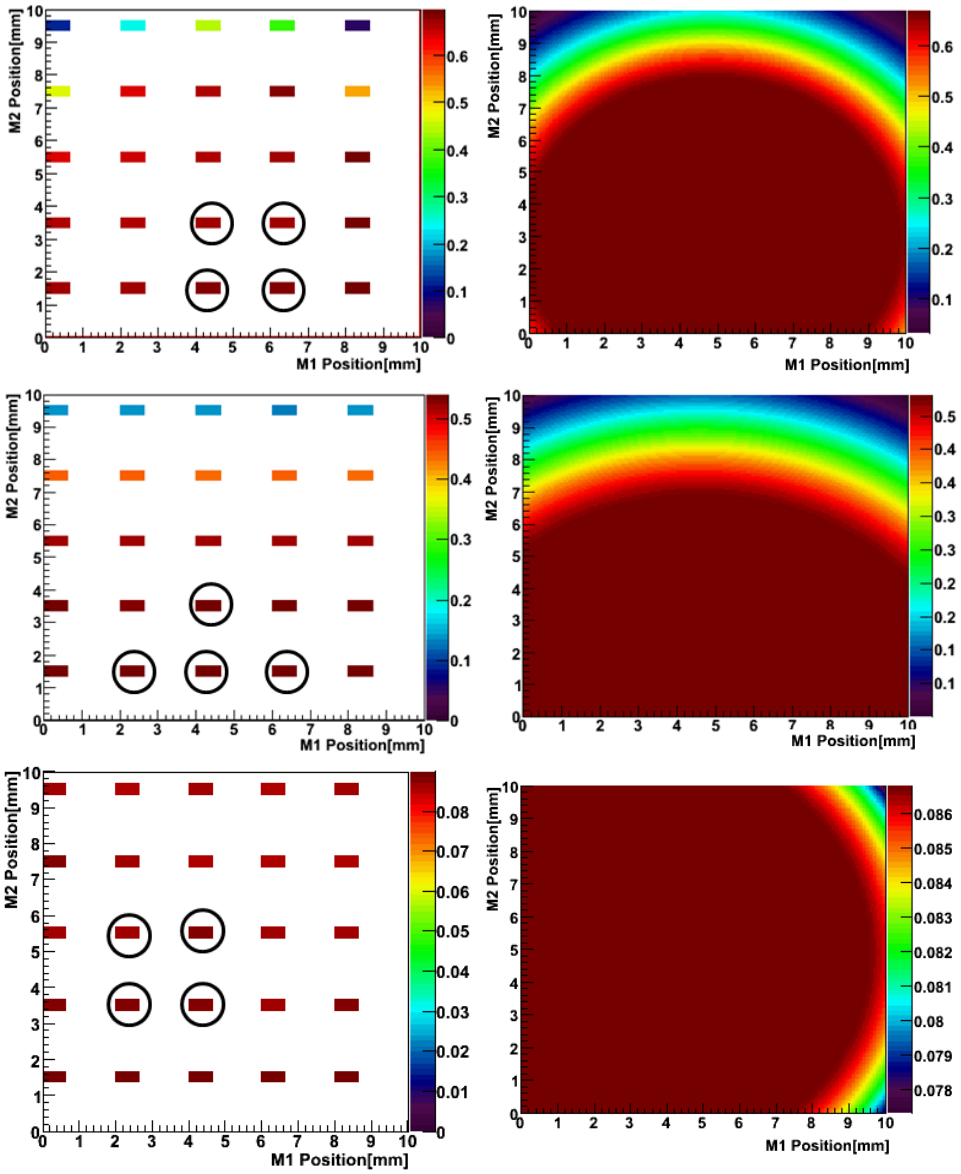

Figure 9: Conversion factor maps (left plots) with the 4 closest points to the center (black circles) and associated fitted plateau-Gaussian function (right plots) for respectively the injection, reflection and transmission VP for the calibration of May 2009.

VP	start GPS	$\Delta t(s)$	I(A)
Inj	925724080	460	1.0
Inj	925725000	460	2.0
Inj	925726218	454	2.35
Inj	925727240	460	1.5
Ref	925737195	460	1.0
Ref	925737830	420	2.0
Tra	925740680	460	1.0
Tra	925741265	460	2.0

Table 7: Configuration for each scan performed in May 2009.

Conversion Factor	Fit	4 Points	1 Point
α_{inj}(W/V)	0.6523±0.0031	0.6590±0.0032	0.6473±0.0032
α_{ref}(W/V)	0.5293±0.0033	0.5368±0.0034	0.5409±0.0035
α_{tra}(W/V)	0.0852±0.0005	0.0856±0.0005	0.0852±0.0005
Losses	0.0712±0.0098	0.0682±0.0098	0.0392±0.0099

Table 8: May 2009 averaged conversion factors for each VPs from the 3 methods presented in section 3.2, corrected by the VPs transmitivity and non-symmetrized.

VP	Scan	I(A)	x_{center}[mm]	y_{center}[mm]	$R_{plateau}$[mm]	$\alpha_0^{'}$[W/V]	w[mm]
Injection	0	1.0	4.860±0.107	2.926±0.068	4.745±0.090	0.6685±0.0003	2.278±0.074
Injection	1	2.0	5.004±0.132	2.828±0.104	4.855±0.107	0.6547±0.0003	2.413±0.246
Injection	2	2.4	4.914±0.077	2.927±0.065	4.692±0.068	0.6533±0.0004	2.335±0.220
Injection	3	1.5	4.902±0.108	2.898±0.079	4.775±0.094	0.6583±0.0003	2.341±0.180
Reflection	0	1.0	4.604±0.014	0.000±0.001	6.574±0.013	0.5303±0.0002	3.100±0.016
Reflection	1	2.0	4.000±0.000	0.000±0.000	6.988±0.012	0.5216±0.0001	2.468±0.014
Transmission	0	1.0	3.014±1.947	4.890±5.142	6.330±2.236	0.0868±0.0001	6.730±5.424
Transmission	1	2.0	3.172±2.339	4.788±1.735	6.235±1.275	0.0833±0.0000	6.702±8.272

Table 9: Result of the plateau gaussian function fit for the calibration performed in May 2009. The parameter errors are given by the fit.

3.3.2 January 2010

The laser power level was controlled via the *Ca_NI_Photon* channel as described in subsection 2.3. In average, each positions is measured during $20 - 3 = 17$ seconds.

For each VP and before injections, offsets in the photodiode and the powermeter was measured (cf. table 10). To do it, the residual laser beam (i.e *Ca_NI_Photon*=0.0V) has been cut with a beam dump (zone A on figures 10). A zero set command has also been sent to the powermeter during this period (represented by the letter B on these figures). The photodiode offsets are measured inside the zone represented by the letter C. The powermeter offsets are measured during the same period for the reflection and transmission. At the injection and inside the zone A, the power measured seems to decrease and cannot be used for an offset measurement. Therefore, it is measured after when the laser beam is back because the signal is more stable. In return the power offset for the injection is likely overestimated.

Laser powers used for the scans are summarized in table 11. Typical map $\alpha^{'}(R)$ and corresponding fit, associated to a beam scan for each VP is shown figure 11 and fits results of each scan are shown in table 13. Boundaries of the plateau are more visible than in May which implies a better accuracy on fits. This is probably due to a better tuning of the distance between the lens and the powermeter as well as a better alignement of the powermeter. Table 12 shows (α_{inj} ,α_{ref}, α_{tra}) for January 2010 and the corresponding losses, for the three methods.

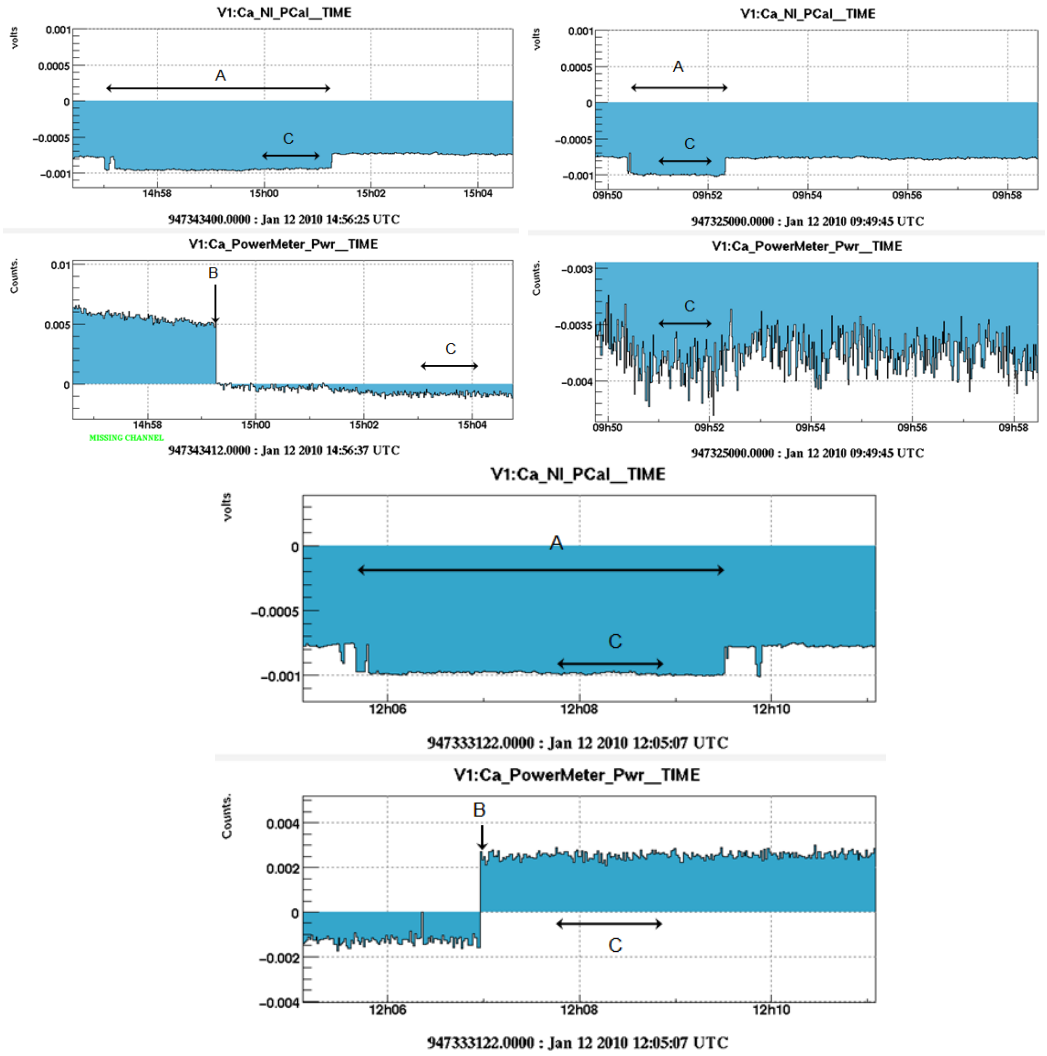

Figure 10: Photodiode and powermeter level when the PCal beam is cut at the injection and reflection (on left and rigth top plots) and at transmission (on bottom plot).

Measurement location	start GPS	Δt(s)	$P_0^{'}(mW)$	Ca_0(mV)
Injection	947343615	60	-	-0.94±0.06
Injection	947343800	60	-0.81±0.17	-
Reflection	947325075	60	-3.87±0.17	-1.0±0.05
Transmission	947333276	100	2.54±0.17	-0.99±0.05

Table 10: Powermeter ($P_0^{'}$) and Photodiode (Ca_0) offsets measured at the injection, reflection and transmission in January 2010.

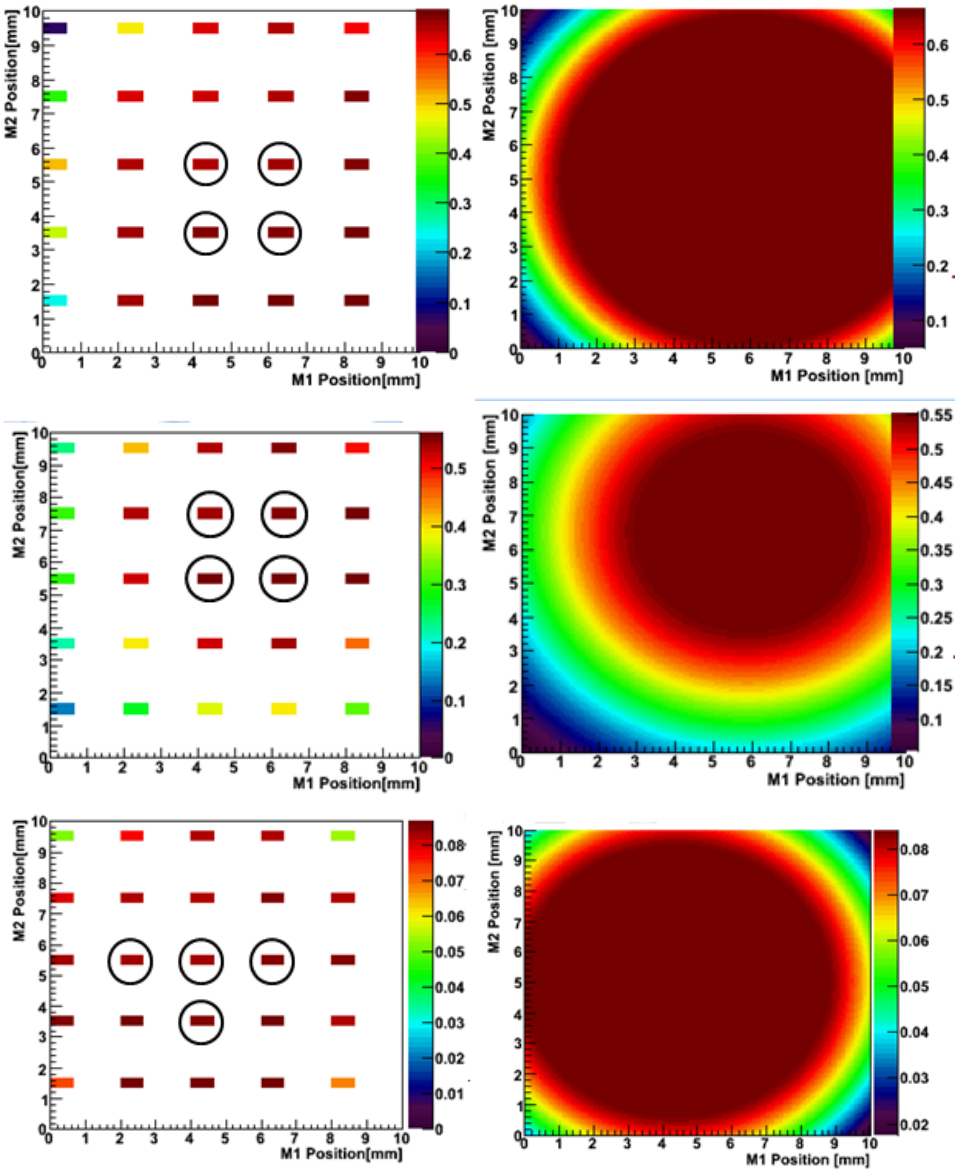

Figure 11: Conversion factor maps (left plots) with the 4 closest points to the center (black circles) and associated fitted plateau-Gaussian function (right plots) for respectively the injection, reflection and transmission VP for the calibration of January 2010.

VP	start GPS	Δt(s)	Ca_NI_Photon(V)
Inj	947345220	735	1.0
Inj	947349525	750	2.0
Inj	947346890	865	3.0
Inj	947347934	840	4.0
Ref	947325733	460	1.0
Ref	947326595	420	3.0
Ref	947327595	460	5.0
Tra	947333690	720	1.0
Tra	947334730	1470	3.0
Tra	947337758	840	5.0

Table 11: Configuration for each scan performed in January 2010.

Conversion Factor	Fit	4 Points	1 Point
α_{inj}(W/V)	0.6394±0.0030	0.6500±0.0031	0.6490±0.0031
α_{ref}(W/V)	0.5557±0.0035	0.5489±0.0035	0.5591±0.0036
α_{tra}(W/V)	0.0809±0.0005	0.0809±0.0005	0.0801±0.0005
Losses	0.0049±0.0092	0.0368±0.0064	0.0174±0.0094

Table 12: January 2010 averaged conversion factors for each VPs from the three methods presented in section 3.2 corrected by the VPs transmitivity and non-symmetrized.

VP	Scan	Ca_NI_Photon[V]	x_{center}[mm]	y_{center}[mm]	$R_{plateau}$[mm]	$\alpha_0^{'}$[W/V]	w[mm]
Injection	0	1.0	5.954±0.008	4.962±0.006	4.646±0.010	0.6621±0.0004	1.943±0.014
Injection	1	2.0	6.291±0.016	4.875±0.005	5.114±0.017	0.6544±0.0002	1.736±0.007
Injection	2	3.0	5.955±0.002	4.944±0.002	4.687±0.003	0.6532±0.0001	1.916±0.004
Injection	3	4.0	6.239±0.010	4.891±0.003	5.073±0.011	0.6386±0.0001	1.757±0.005
Reflection	0	1.0	5.900±0.006	6.512±0.005	2.487±0.011	0.5538±0.0005	4.106±0.015
Reflection	1	3.0	5.882±0.002	6.506±0.002	2.518±0.005	0.5495±0.0002	4.111±0.008
Reflection	2	5.0	5.844±0.002	6.463±0.002	2.436±0.005	0.5470±0.0002	4.181±0.007
Transmission	0	1.0	4.372±0.027	5.025±0.027	4.195±0.056	0.0842±0.0002	2.64912±0.097
Transmission	1	3.0	4.400±0.007	5.050±0.007	4.199±0.015	0.0812±0.0001	2.643±0.028
Transmission	2	5.0	4.362±0.006	5.055±0.005	4.216±0.013	0.0789±0.0000	2.653±0.023

Table 13: Result of the plateau Gaussian function fits for the calibration performed in January. The parameter errors are given by the fit.

3.4 PCal calibrations synthesis

Because of a better alignment performed in January 2010, $\alpha_{ref,sym}$ extracted by the fit method for this calibration is used as the PCal calibration factor α_{PCal}. The systematic error on the power calibration is obtained with the dispersion of $\alpha_{ref,sym}$ relative to α_{PCal} over the following extraction methods:

- fit method on May 2009 data .
- 4 and 1 points methods on January 2010 and May 2009 data.
- fit method considering $\alpha_{inj,sym}$, $\alpha_{ref,sym}$, $\alpha_{tra,sym}$ extracted from map for which the same level of laser power was injected (For January: 90 and 360 mW, for May: 200 and 600 mW).

The table 14 shows results of this comparison. **For VSR2, the reflection conversion factor is 0.557 and we used a conservative systematic error of 2% for the measurement method (including uncertainties on Viewports and lens transmitivity and power measurement systematic errors)**.

Method	$\alpha_{ref,sym}$	Half losses (%)	Variation to α_{PCal} (%)
Fit (all scans)	**0.557**	**0.2**	**-**
Fit (scans 90 mW)	0.566	0.9	1.5
Fit (scans 360 mW)	0.560	0.7	0.6
4 points	0.559	1.8	0.3
1 point	0.564	0.9	1.2
Fit (all scans)	0.548	3.6	-1.6
Fit (scans 200 mW)	0.555	3.4	-0.4
Fit (scans 600 mW)	0.546	3.4	-2.0
4 points	0.555	3.4	-0.4
1 point	0.551	2.0	-1.0

Table 14: Variation of $\alpha_{ref,sym}$ over different extraction methods relative to the PCal calibration factor α_{PCal}. The top part of the table corresponds to the January calibration and the bottom part, to May.

3.5 Systematic errors on the effective force seen by the mirror

Systematic errors contributing to the force F induced by the PCal on the NI mirror are the geometry and the power calibration uncertainties (cf. equation 1). These values detailed in table 3.5 are respectively 2.5% and 6.5% and leads to a 9% F uncertainty (by linear addition). The sensor head non-uniform response corresponds to the power variation observed when the beam is inside the powermeter sensor. This variation is visible on the maps and has been confirmed by measurements made at LAPP of a 3% difference.

Origin	Uncertainty (± %)
cosine of the incident angle	2.5
Powermeter absolute calibration	3
Sensor head non-uniform response	1.5
PCal power calibration methods	2.0

4 Timing of the photodiode

The IRIG-B signal used to encode the GPS time is used here to measure the delay of the PCal photodiode readout. The IRIG-B signal is built by the GPS receiver and sent through optical fiber to Timing Distribution Box of the detection crate. The propagation time has been measured and is 16.041μs ([5]). It has been then sent through a 27 meters cable to a red LED placed in front of the PCal photodiode and the signal is measured by the photodiode and stored in the channel Ca_NI_PCal. The propagation time in this cable is 150 ns.
The standard readout of the photodiode is constituted of (see figure 12):

- the photodiode itself.
- a 30 meter coaxial cable (propagation time is 135 ns ibn this cable).
- the analog readout eletronics where the current sent by the photodiode is read and converted in voltage (analog electronics).
- an anti-alias filter (+6.61 μs delay) on a mezzanine (serial number 638) of the ADC board.
- a sampling operation at 800 kHz in the ADC.
- a 8th order digital Butterworth filter (fc=7503.65Hz) equivalent to a +109 ($\pm$ 1.0) μs delay below 1kHz.
- an under sampling operation at 20 kHz (-48.75 μs delay).
- a GPS assignement in the DAQ (-16.041 μs delay). This comes mainly from the IRIG-B propagation time in optical fiber between the GPS receiver and the ADC in Virgo (3350 m).

There were two measurements performed with the LED in front of the photodiode:

- *Ca_NI_PCal* read at GPS 947358400 during 60 seconds at 20 kHz with the previous configuration(left path on the figure 12).
- *Ca_NI_PCal* read at GPS 947358480, for 60 seconds at 800 kHz without digital filtering and no undersampling (right path on the figure 12).

By comparing the start of the frame with the rise time of the IRIG-B 1 PPS signal in the Ca_NI_PCal channel, we estimate :

- the delay $d_{box+photodiode}$ introduced by the photodiode and the analog readout eletronics.

- the presence of additional delay in the numerical filtering.

For the standard path, the rise time occurs between 50 and 100μs after the frame start (cf. figure 13) and the expected delay(below 1 kHz) is 16.04 + 0.135 + 0.11 + $d_{box+photodiode}$ + 6.61 + 109.0($\pm$1) - 48.75 - 16.04 = 67.1 ($\pm$1) μs + $d_{box+photodiode}$.
At 800 kHz path, the expected delay is 16.04 + 0.15 + 0.11 + $d_{box+photodiode}$ + 6.61 - 16.04= 6.87 μs + $d_{box+photodiode}$ and the rise is significative between the 5^{th} and 6^{th} sample from the frame start which leads to a delay range from $5 \times \frac{1}{800000Hz} = 6.25\mu s$ to $6 \times \frac{1}{800000Hz} = 7.5\mu s$. In both situations, expectations and measurements are compatible within uncertainties (dominated by the signals sampling frequency).

We conclude from the 800kHz path that the delay introduced by the photodiode+analog readout eletronics is less than 1μs and is estimated to 0.5$\pm$0.5 μs. The absolute delay of channel *Ca_NI_PCal* with respect to GPS time is then:

- 0.5$\pm$0.5 + 0.15 + 6.61 + 109$\pm$1.0 - 48.75 - 16.04 = 51.47$\pm$1.5 μs below 1kHz
- 0.5$\pm$0.5 + 0.15 + 6.61 + $d_{Butterworth}$- 48.75 - 16.04 = -57.53$\pm$0.5μs + $d_{Butterworth}$. $d_{Butterworth}$ is the frequency dependant delay introduced by the Butterworth filter (model valid up to 10kHz).

The 4 μs systematic error on Virgo absolute timing ([6]) has to be taken into account as *Ca_NI_PCal* timing systematic errors.

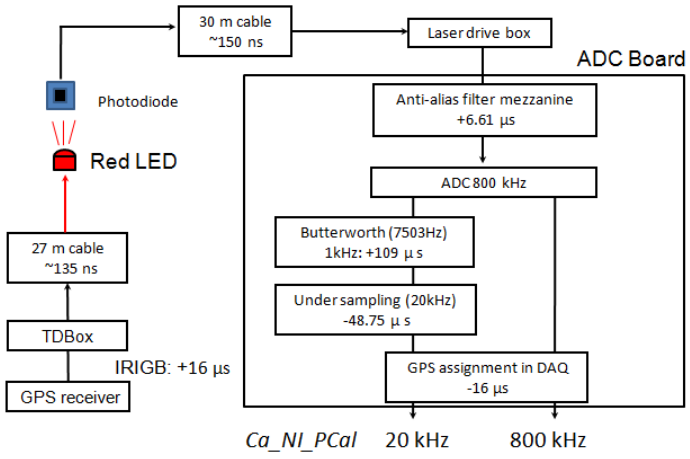

Figure 12: Overview of the photodiode readout for the conventional and non filtered path.

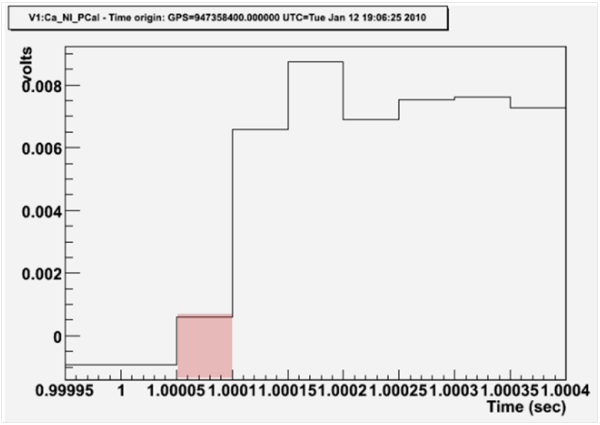

Figure 13: Rise time of the IRIG-B signal at the ouput of the photodiode sampled at 20 kHz. The rise time is seen in the 2th sample after frame start (red rectangle).

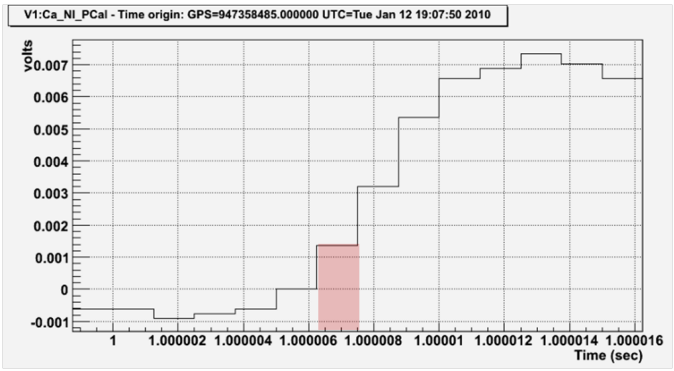

Figure 14: Rise time of the IRIG-B signal at the ouput of the photodiode sampled at 800 kHz. The rise time is seen in the 6th sample after frame start and is represented by the red rectangle.

5 Conclusion

The Photon Calibrator has been installed on the North input arm before VSR2. The setup has been characterized through the laser beam power saturation, the timing of the monitoring photodiode and the viewports transmitivity measurement. The PCal power calibration for VSR2 takes into account two calibrations performed in May 2009 and January 2010. The power calibration is determined with the January calibration which is more accurate. The systematic error of the PCal power calibration is 6.5% and the mirror longitudinal motion one, including geometrical uncertainties, is estimated to 9%. The timing of the photodiode readout has been done with a delay estimated at $+51.43 \pm 4.5$ μs below 1000Hz.

References

[1] T. Accadia, L. Rolland, B. Mours *h reconstruction characterization with the Photon Calibrator*, in preparation.

[2] O. Veziant, Thèse de l'Université de Savoie, *Calibration de l'expérience VIRGO, de l'étalonnage du détecteur à la recherche de signaux de coalescences binaires avec l'interféromètre VIRGO*(2003).

[3] L. Rolland, F. Marion, B. Mours, *Use of the Photon Calibrators for the VSR1 calibration*, VIR-053A-08 (2008).

[4] Virgo working area web page: https://workarea.ego-gw.it/ego2/virgo/data-analysis/calibration-reconstruction/auth-only/optical-calibrator/hardware-list/ .

[5] N. Letendre, A. Masserot, B. Mours, *Virgo+ Timing Deployment*, VIR-073B-08 (2008).

[6] L. Rolland, *Calibration status in September 2009*, VIR-0576A-09 (2009).